Stochastic Optimization for Energy Management in Power Systems With Multiple Microgrids

Shasha Wang, Harsha Gangammanavar, Sandra D. Ekşioğlu, and Scott J. Mason

***Abstract*—This paper is motivated by a power system with one main grid (arbiter) and multiple microgrids (MGs) (agents). The MGs are equipped to control their local generation and demands in the presence of uncertain renewable generation and heterogeneous energy management settings. We propose an extension to the classical two-stage stochastic programming model to capture these interactions by modeling the arbiter's problem as the first-stage master problem and the agent decision problems as second-stage subproblems. To tackle this problem formulation, we propose a sequential sampling-based optimization algorithm that does not require *a priori* knowledge of probability distribution functions or selection of samples for renewable generation. The subproblems capture the details of different energy management settings employed at the agent MGs to control heating, ventilation, and air conditioning systems, home appliances, industrial production, plug-in electrical vehicles, and storage devices. Our computational experiments conducted on the U.S. western interconnect (WECC-240) data set illustrate that the proposed algorithm is scalable and the solutions are statistically verifiable. Our results also show that the proposed framework can be used as a systematic tool to gauge: 1) the impact of energy management settings in efficiently utilizing renewable generation and 2) the role of flexible demands in reducing system costs.**

***Index Terms*—Microgrids, energy management, demand response, multi-agent stochastic optimization, stochastic decomposition.**

NOMENCLATURE

Sets

$\mathcal{N}$	$:= \{0, 1, 2, \ldots, N\}$, the set of agents ($n = 0$ is the main grid)
$\mathcal{T}$	$:= \{0, 1, 2, \ldots, T\}$, set of discrete time decision epochs.

In the following definitions, $t \in \mathcal{T}, n \in \mathcal{N}$ will hold, unless otherwise mentioned.

$\mathcal{B}_n$	buses
$\mathcal{L}_n$	transmission lines
$\mathcal{I}_n$	interconnection lines connected the main grid and microgrid n, $n \in \mathcal{N} \setminus \{0\}$
$\mathcal{G}_n$	conventional generators
$\mathcal{R}_n$	renewable generators
$\mathcal{D}_n$	demands
$\mathcal{D}_n^f$	fixed demands
$\mathcal{D}_n^v$	flexible demands
$\mathcal{V}_n^i$	industrial facilities
$\mathcal{V}_n^h$	buildings that have heating, ventilation, and air conditioning systems
$\mathcal{V}_n^b$	storage devices
$\mathcal{V}_n^p$	plug-in electrical vehicles
$\mathcal{V}_n^a$	home appliances.

Subset $\mathcal{G}_{ni} \subseteq \mathcal{G}_n$ denotes conventional generators connected to bus $i \in \mathcal{B}_n$. Similarly, we have the subsets $\mathcal{R}_{ni}$ and $\mathcal{D}_{ni}$.

Parameters

D_{njt}	fixed demand (MW), $j \in \mathcal{V}_n^f$
D_j^i	total flexible demands (MW) required by industrial facility, $j \in \mathcal{V}_n^i$
D_j^a	total flexible demands (MW) required by home appliances, $j \in \mathcal{V}_n^a$
D_{jt}^h	minimum level of demand (MW) required by heating, ventilation, and air conditioning system $j \in \mathcal{V}_n^h$
Δ_{jt}^h	flexible portion of demand (MW) adapted by heating, ventilation, and air conditioning system, $j \in \mathcal{V}_n^h$
S_j	total demand required by PEV, $j \in \mathcal{V}_n^p$
c_{njt}^g	conventional generation cost per MW, $j \in \mathcal{G}_n$
c_{ijt}^b	selling price of power per MW, $(i, j) \in \mathcal{I}_n$
d_{ijt}^p	penalty for under-utilizing the power already purchased (per MW), $(i, j) \in \mathcal{I}_n$
d_{nit}^r	penalty for under-utilizing the renewable power (per MW), $i \in \mathcal{R}_n$
d_{nit}^ℓ	penalty for unmet demand (per MW), $i \in \mathcal{D}_n$
$\mathcal{A}_n^v$	feasible region for decisions a_{njt}
V_{nit}	voltage of bus $i \in \mathcal{B}_n$
X_{nij}	reactance of line $(i, j) \in \mathcal{L}_n$
v_n	weight of agent n
a_j^{min}, a_j^{max}	bounds of utilized power (MW), $j \in \mathcal{D}_n$
s_j^{min}, s_j^{max}	bounds of charging/discharging activities for storage devices and plug-in electrical vehicles (MW), $j \in \mathcal{V}_n^b \cup \mathcal{V}_n^p$
$p_{nij}^{min}, p_{nij}^{max}$	bounds of power flow (MW) distributed by line $(i, j) \in \mathcal{L}_n$
$[\underline{\tau}_j^i, \bar{\tau}_j^i] \subseteq \mathcal{T}$	operation time interval for industrial facility $j \in \mathcal{V}_n^i$

Manuscript received March 18, 2017; revised June 26, 2017 and August 18, 2017; accepted September 17, 2017. Date of publication October 3, 2017; date of current version December 19, 2018. Paper no. TSG-00378-2017. *(Corresponding author: Shasha Wang.)*

S. Wang, S. D. Ekşioğlu, and S. J. Mason are with the Industrial Engineering Department, Clemson University, Clemson, SC 29634-0002 USA (e-mail: shashaw@g.clemson.edu).

H. Gangammanavar is with the Engineering Management, Information, and Systems Department, Southern Methodist University, Dallas, TX 75205 USA.

Color versions of one or more of the figures in this paper are available online at http://ieeexplore.ieee.org.

Digital Object Identifier 10.1109/TSG.2017.2759159

$[\underline{\tau}_j^p, \bar{\tau}_j^p] \subseteq \mathcal{T}$ operation time interval for plug-in electrical vehicle $j \in \mathcal{V}_n^p$

$[\underline{\tau}_j^a, \bar{\tau}_j^a] \subseteq \mathcal{T}$ operation time interval for home appliance $j \in \mathcal{V}_n^a$

$\tilde{\omega}_{njt}$ random variable, renewable generation (MW), $j \in \mathcal{R}_{ni}$.

Decision Variables

b_{ijt} transaction power (MW) between the main grid and micogrid n, $(i,j) \in \mathcal{I}_n$, $n \in \mathcal{N} \setminus \{0\}$

g_{njt} conventional generation level (MW) at main grid, $j \in \mathcal{G}_n$

a_{njt} power (MW) utilized to meet demand, $j \in \mathcal{D}_n$

s_{njt} state of storage devices/plug-in electrical vehicles, $j \in \mathcal{V}_n^b \cup \mathcal{V}_n^p$

p_{nijt} power flow (MW) distributed by line $(i,j) \in \mathcal{L}_n$

u_{jit}^p unused purchased power (MW), $(j,i) \in \mathcal{I}_n$

u_{nit}^r unused renewable generation (MW), $i \in \mathcal{R}_n$

u_{nit}^ℓ unmet demand (MW), $i \in \mathcal{D}_n$

θ_{nit} voltage angle of bus $i \in \mathcal{B}_n$.

I. Introduction

MICROGRIDS have recently emerged as an alternative for reducing greenhouse gas emissions and transmission losses [1], [2]. A microgrid (MG) is a small-scale power grid that is comprised of distributed energy resource systems, storage devices, local demands, and a distribution network [3], [4]. The capacity of such a distributed energy resource system varies from 1500 kW to 1000 MW, which is smaller than a centralized conventional power station [5]. Among all distributed energy resources used in MGs, renewable energy sources (RESs), such as wind and solar, have obtained more attention. Besides reducing greenhouse gas emissions, RESs are easy and economical to obtain, especially in islands and outermost regions [6]. Many researchers have investigated methods to increase the penetration of RESs in MGs such as using storage devices [7]. However, the inherent stochasticity of renewable resources, such as wind and solar, introduces operational challenges of MGs.

An attractive feature of MGs is their ability to operate both as part of a larger power grid [8], [9] as well as in an islanded mode [6], [10]. MGs can transact power with the larger grid when they are connected, thereby acting as a source/sink for deficient/excess power in the system. In times of stress, such as during a storm or service interruption, an MG can break off from the larger grid and operate independently on its own. These capabilities can provide additional reliability options to power system operations. Energy managers [3] at microgrids make generation decisions according to information provided by local generation capacity, customer demand, and the amount of power transacted with the main grid.

For these reasons, there has been a growing number of publications that focus on the operations of MGs in the presence of renewable energy resources and/or storage devices. These works have attempted to capture the interactions between MGs and system operators. The setting in [8] was addressed using a simulation-based testing method where economic dispatch decisions at MGs are solved in a primary level and a secondary level optimization seeks to minimize overall operating costs. In [9], TSO-DSO-MGs interactions are captured via an optimization problem that is solved using diagonal quadratic approximation method and a variant of alternating directions method of multipliers. Networked MGs using a bi-level programming model were presented in [11]. A deterministic equivalent mathematical program with complementarity constraints of the bi-level program built using a scenario reduction technique is proposed as a solution approach. In these studies, authors attempt to optimize all MGs simultaneously, which can result in a large optimization problem. In order to achieve computational viability, they consider only a small number of MGs in the system and resort to a limited sample representation of uncertainty. However, it is expected that in the future, the main grid will interact with a large number of MGs. Alternatively, energy management in a multi-agent setting and in the context of electricity markets has been studied by [12]–[14]. These problems are solved using agent-oriented programming, Lagrangian-relaxation genetic algorithms, and a combination of stochastic programming and game theory, respectively. Once again, these works are limited to a small set of MGs to achieve computational viability. Moreover, developing solution approaches that converge in uncertain problem settings is still an area of active research. We adopt a stochastic programming approach to tackle some of these issues. Stochastic programming has previously been applied successfully to power system operation problems as they provide convenient tools to model complicated interactions, physical restrictions, and uncertainties [15]. In our work, we propose a novel approach to model this multi-agent setup and a sequential sampling algorithm to solve this problem, which provide provably convergent solutions.

MGs allow integrating smart grid control systems and innovative energy management technologies with traditional operations. In a smart grid, customers are allowed to adjust their energy consumption according to real-time electricity prices. The adjustable appliances either have flexible ranges of power demand or can shift their demand between periods. This behavior, which is called demand response, brings operational flexibility while imposing newer challenges on energy management systems. Most of adjustable demands considered in literature are storage devices and plug-in electrical vehicles [7], [16], [17]. Marzband *et al.* [8] and Nguyen and Le [17] provide mathematical models for general adjustable demand. However, the type of adjustable demands varies including industrial, commercial, and residential. Reference [18] studies non-schedulable and schedulable tasks in industrial facilities. Reference [19] studies heating, ventilation, and air conditioning demand response control in commercial buildings. Reference [20] presents detailed models of appliances commonly used in households and investigates the optimal demand response schedule that maximizes customer's net benefit. Reference [21] proposes stochastic optimization and robust optimization approaches for real-time price-based demand response management for residential appliances. In this work, we propose a detailed mathematical model that captures heterogeneous management systems with

adjustable demands and incorporates physical power network restrictions.

In light of the above contents, the main contributions of this paper are:

1) A stochastic programming model that extends the classical two-stage formulation to accommodate multiple subproblems. In the power systems context, this model is designed for a centralized arbiter, who is charged with generating and supplying power to a set of utilities and MGs with various weights (priorities), in the main grid. Each MG is allowed to respond to the decision of the centralized arbiter and a stochastic realization of renewable generation.
2) A comprehensive model that allows MGs to use different energy management systems. This leads to heterogeneous agent optimization problems, operating time periods, and stochastic processes. To the best of our knowledge, our work is the first to consider such a setup.
3) An extension of the two-stage stochastic decomposition (2-SD) to solve models with multiple subproblems. Our approach, which we refer to as the multi-agent stochastic decomposition, is a decomposition-based sequential sampling algorithm. It dynamically identifies the number of samples required to characterize the uncertainty at a particular MG and provides statistically verifiable solutions and objective function estimates.
4) A comprehensive computational analysis that highlights the scalability of the proposed algorithm to large-scale power systems. The results of our analysis illustrate the performance of the algorithm, the benefits of energy management systems, and the advantages of flexible demands.

The remainder of the paper is organized as follows. In Section II, the energy management in power systems is studied and corresponding mathematical model is presented. The multi-agent stochastic decomposition is implemented in Section III. Computational experiments are conducted in Section IV. Finally, conclusions are offered in Section V.

II. Problem Formulation

We consider a power system that is comprised of a main grid connected to multiple agents. The main grid can either be a transmission or distribution network. In transmission networks, the independent system operator (ISO) acts as the centralized arbiter bestowed with the responsibility of managing not only the operations (generation, transmission, etc.) of the transmission network, but also managing the transactions with distribution networks and MGs connected to it. The agents themselves are managed by autonomous decision-making entities (distribution system operators (DSO) for distribution networks and energy management systems for MGs). Similarly, the distribution system operator shares the same interactions with MGs connected to the distribution network. While the role of decision makers at individual agents is concerned with the operations on a small/local scale, the centralized arbiter is interested in optimal operations of the entire system. The formulation presented in this section encompasses any such relationship between the centralized arbiter and agents. In the remainder of the paper, we will restrict all agents to be MGs with independent energy management systems controlling their operations.

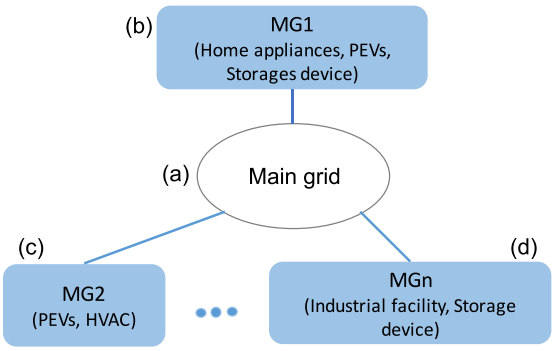

Fig. 1. A power system: A main grid (a) connects to multiple MGs ((b) - (d)) that utilize different energy management settings

The power system uses both conventional and renewable energy resources to meet customer demands. Each entity in the system is exposed to varied sources of uncertainty (demand, renewable generation, etc.) and utilizes different energy management settings. Fig. 1 shows the system we described above. To capture these properties of the system, we present a stochastic optimization formulation that is comprised of (a) an arbiter problem where decisions are made before the realization of any uncertainty and (b) multiple agent problems where decisions are made in response to their respective stochastic outcomes. This formulation is an extension of the classical 2-SP and will be referred to as the multi-agent stochastic program (MA-SP). At time period t, customer demands at each agent can be met through local generation (conventional and renewable) as well as energy bought from the main grid (when $n \neq 0$). We first begin by presenting the arbiter's optimization problem.

A. Arbiter Problem

The centralized arbiter determines the conventional generation level at the main grid as well as its power transactions with all the MGs. The set of generators in the main grid is denoted by $\mathcal{G}_0$. For every generator $j \in \mathcal{G}_0$, the generation level and the corresponding cost are denoted by g_{0jt} and c^g_{0jt}, respectively. The transaction decisions b_{ijt} between the main grid and MGs are determined for all $(i,j) \in \mathcal{I}_n$ at a price of c^b_{ijt}, where $\mathcal{I}_n$ is the set of interconnection links. These generation and transaction decisions are made so as to satisfy the following power balance equation:

$$\sum_{j\in\mathcal{G}_0} g_{0jt} = \sum_{j\in\mathcal{D}_0\bigcup\mathcal{R}_0} \partial\bar{D}_{0jt} + \sum_{(i,j)\in\mathcal{I}_n} b_{ijt} \quad \forall t \in \mathcal{T}, \qquad (1)$$

where $\partial\bar{D}_{0jt}$ is the net demand computed using the forecasted demand ($\mathcal{D}_0$) and renewable generation ($\mathcal{R}_0$) in the main grid. In addition, generation and transaction decisions are bounded by their respective physical limits. Further, these decisions are established in a "here and now" manner and effect the state of every agent in the system. We will succinctly denote the

arbiter's decision vector by $x = (x_t)_{t\in\mathcal{T}}$ and cost vector by $c = (c_t)_{t\in\mathcal{T}}$, where $x_t = ((g_{0jt})_{j\in\mathcal{G}_0}, (b_{ijt})_{(i,j)\in\mathcal{I}})$ and the corresponding cost coefficients by $c_t = ((c^g_{0jt})_{j\in\mathcal{G}_0}, (-c^b_{ijt})_{(i,j)\in\mathcal{I}})$. The feasible set characterised by (1) is denoted by $\mathcal{X}$. Once the arbiter makes its decision, each agent responds to this decision and a realization ω_n of its stochastic process $\tilde{\omega}_n$ at a recourse cost of $h_n(x, \omega_n)$. We assume that the stochastic processes affecting the agents are independent of each other.

The objective of the centralized arbiter is to minimize the energy cost and the sum of weighted expected recourse functions. Its optimization problem is given by:

$$\begin{aligned} \min\ & c^\top x + \sum_{n\in\mathcal{N}} v_n \mathbb{E}\{h_n(x, \omega_n)\} \\ \text{s.t.}\ & x \in \mathcal{X}, \end{aligned} \tag{2}$$

where the weight $v_n \geq 0\ \forall n \in \mathcal{N}$ is chosen based on the relative preference of the agents set by the centralized arbiter. For example, an agent with critical infrastructures (like hospitals) has higher priority (weight) than other agents.

B. Agent Problem

Each agent in the system, that is, the main grid and all MGs, is associated with an agent problem. This problem is characterized by the energy management setting adopted and stochasticity faced by the agent. The energy resources of an agent n include the set of conventional generators $\mathcal{G}_n$ as well as renewable generators $\mathcal{R}_n$. The conventional generators at MGs ($n \neq 0$) usually have lower capacities when compared to the main grid ($n = 0$) generators. In addition to these local energy resources, the MGs can utilize a fraction of the energy available from the main grid. The generation levels $g_{0jt}\ \forall j \in \mathcal{G}_0$ at the main grid, which were set by the arbiter, are allowed to be updated.

These resources are used to meet customers demands, which are denoted by $\mathcal{D}_n$. Further, all customer demands can be categorized as fixed and flexible. The fixed demand, D_{njt}, at location $j \in \mathcal{D}^f_n$ must be met in the current time period t. In other words,

$$a_{njt} \geq D_{njt}, \tag{3}$$

where a_{njt} is the power utilized to meet this fixed demand. The flexible demand, $\mathcal{D}^v_n$, depends on the energy management settings adopted by each agent. We will describe these settings in the following.

1) Energy Management Settings: Each agent may adopt (one or more) different settings. Therefore, we omit the agent index n while presenting these settings.

1) *Industrial Sector:* The field of production management provides flexibility in how demand at a particular facility can be met during the operation time horizon [18]. This, in turn, allows for efficiently utilizing the available energy resources. To ensure that the production demand is met, the cumulative power consumption within a production window must exceed a given threshold. Let $\mathcal{V}^i$ denote a set of industrial facilities. If for each $j \in \mathcal{V}^i$, the time window within which the demand D^i_j can be satisfied is given by $[\underline{\tau}^i_j, \bar{\tau}^i_j] \subseteq \mathcal{T}$. This requirement is captured by:

$$\sum_{t\in[\underline{\tau}^i_j, \bar{\tau}^i_j]} a_{jt} \geq D^i_j. \tag{4}$$

In the above, a_{jt} is the realized power in time period t that is restricted to be within an interval $[a^{min}_j, a^{max}_j] \in \mathbb{R}$. The equipment used in industrial settings is associated with significant start-up time and set-up cost. Therefore, it is efficient to run the industrial equipment uninterrupted, which is ensured by setting $a^{min}_j > 0$.

2) *Building Management:* For commercial buildings, around 50% of the energy is consumed by heating, ventilation, and air conditioning (HVAC) systems to provide a comfortable indoor environment [22]. Let $\mathcal{V}^h$ denote the set of buildings that have intelligent HVAC systems. Since comfort is a qualitative term, it is best captured through a flexible range. For example, the comfortable indoor temperature ranges between 20°C to 25°C [23]. Moreover, this comfort is also associated with climate [24] and building occupancy [25]. For these reasons, the amount of energy consumed has a fixed minimum level D^h_{jt} (corresponding to the minimum comfort requirement) and a flexible portion Δ^h_{jt} for all $j \in \mathcal{V}^h$. The flexible portion can frequently fluctuate within a range without reducing the end-user's comfort significantly. This is ensured by:

$$D^h_{jt} \leq a_{jt} \leq D^h_{jt} + \Delta^h_{jt} \quad \forall j \in \mathcal{V}^h,\ \forall t \in \mathcal{T}. \tag{5}$$

Note that, while the demand in (4) can be met across multiple time periods, the demand here is time-dependent and should be met in its time period.

3) *Storage Devices:* It has been identified that storage devices will play a critical role in mitigating renewable regulation challenges [26], [27]. Apart from energy arbitrage, storage devices can provide ancillary services, capacity deferral services, and end-user services [28]. Let $\mathcal{V}^b$ denote a set of storage devices. For each $j \in \mathcal{V}^b$, a_{jt} is the charging/discharging amount during time period t. If this value is positive, it indicates a charging activity—discharging otherwise. These decisions are bounded by charging/discharging rates of the storage devices: $a_{jt} \in [a^{min}_j, a^{max}_j] \in \mathbb{R}$. Let s_{jt} denote the state of storage devices that is required to satisfy the following dynamics equation:

$$s_{jt} = s_{j,t-1} + a_{jt} \qquad \forall j \in \mathcal{V}^b,\ \forall t \in \mathcal{T}, \tag{6}$$

where the initial state s_{j0} is assumed to be given. This variable is also bounded by the capacity of this storage device, that is $0 \leq s_{jt} \leq s^{max}_j$. In any time period, a storage device can act both as source and sink of energy.

4) *Plug-in Electric Vehicle (PEV):* The operating principle of PEVs is similar to that of storage devices. However, unlike the storage devices, the charging and discharging activities depend on the utility of the vehicle. For example, it should be expected that the PEVs are connected to a residential grid during the off-work hours. Therefore,

the whole operation must be completed during a time period that is desired by the customer. Using similar definitions as given for storage devices, for $j \in \mathcal{V}_p$, the set of PEVs must satisfy:

$$a_j^{min} \le a_{jt} \le a_j^{max},\ s_j^{min} \le s_{jt} \le s_j^{max}, \tag{7a}$$

$$s_{jt} = s_{j,t-1} + a_{jt} \quad \forall t \in [\underline{\tau}_j^p, \bar{\tau}_j^p], \tag{7b}$$

where $[\underline{\tau}_j^p, \bar{\tau}_j^p]$ is the plug-in interval. Further, the state of the PEVs at the end of the plug-in interval must satisfy the specific customer-desired requirement [21]:

$$s_{j\bar{\tau}_j^p} = S_j \quad \forall j \in \mathcal{V}^p. \tag{8}$$

5) *Home Appliances:* The operation of some appliances, such as dishwashers and washing machines, is flexible over a time horizon. These appliances have relatively lower demand compared to the other settings described thus far. Let $\mathcal{V}^a$ denote a set of appliances. For each $j \in \mathcal{V}^a$, a_{jt} is the power utilized in time period t that must satisfy:

$$\sum_{t \in [\underline{\tau}_j^a, \bar{\tau}_j^a]} a_{jt} \ge D_j^a \tag{9}$$

during the desired time window $[\underline{\tau}_j^a, \bar{\tau}_j^a]$. The operation of these appliances can withstand interruptions since the start-up time and set-up cost are negligible. Moreover, power utilized in any time period should be less than the power rating of the appliance. Therefore, $a_{jt} \in [0, a_j^{max}]$. The interruptible nature of these appliances differentiates them from industrial equipment.

We restrict our attention to the above five settings, but other similar settings can also be operated within our multi-agent framework. Moreover, for agent n the flexible demand set $\mathcal{D}_n^v$ can be any combination of the above settings. The feasible region for decisions a_{njt}, where $j \in \mathcal{D}_n^v$ depends on this combination and will be denoted as $\mathcal{A}_n^v$. For example, for a household with storage devices and PEV units installed, the set $\mathcal{D}_n^v = \mathcal{V}_n^b \bigcup \mathcal{V}_n^p \bigcup \mathcal{V}_n^a$. In this case, the feasible region $\mathcal{A}_n^v$ is characterized by (6), (7), (8), and (9) along with the respective bounds.

2) Power Network Constraints: The power grid in both the main grid and MGs (i.e., for all $n \in \mathcal{N}$) consists of buses and lines that construct a network with a set of buses $\mathcal{B}_n$ and a set of transmission lines $\mathcal{L}_n$. At any bus $i \in \mathcal{B}_n$, the total available power should meet the total of fixed and flexible demands, thus, satisfying the following:

$$\sum_{j \in \mathcal{G}_{ni}} g_{njt} + \left(\sum_{j:(j,i) \in \mathcal{L}_n} p_{njit} - \sum_{j:(i,j) \in \mathcal{L}_n} p_{nijt} \right) - \sum_{j \in \mathcal{D}_{ni}} \left(a_{njt} - u_{njt}^{\ell} \right) = r_i(x_t, \tilde{\omega}_{nit}) \quad \forall t \in \mathcal{T}, \tag{10}$$

where p_{njit} and p_{nijt} are the flow into and out of bus i, respectively. Further, u_{jit} is the purchased power that is unused. Note that this variable appears only in MG problems. The right-hand side $r_i(x_t, \tilde{\omega}_{nit})$ depends on the arbiter's decision and the renewable generation $\tilde{\omega}_{nit}$. Note that the right-hand side $r_i(x_t, \tilde{\omega}_{nit})$ for the main grid and MGs are different since the main grid acts as a seller rather than a buyer in the transactions with agents. Therefore, for any bus $i \in \mathcal{B}_n$, $r_i(x_t, \tilde{\omega}_{nit})$ is set as the following:

$$\left\{ \begin{array}{ll} -\sum_{j \in \mathcal{R}_{ni}} \left(\tilde{\omega}_{njt} - u_{njt}^r \right) + \sum_{j:(i,j) \in \mathcal{I}_n} b_{ijt} & \text{if } n = 0, \\ -\sum_{j \in \mathcal{R}_{ni}} \left(\tilde{\omega}_{njt} - u_{njt}^r \right) - \sum_{j:(j,i) \in \mathcal{I}_n} \left(b_{jit} - u_{jit}^p \right) & \text{if } n \ne 0. \end{array} \right. \tag{11}$$

On any transmission line, the real transmitted power and power losses are non-linear functions of the differences between the voltages and angles of buses in both ends of connecting lines. To make theses functions suitable for linear optimization methods, we apply a linear approximation described in [29]. We ignore the power flow losses. If V_{nit} denotes the voltage of bus i, and X_{nij} denotes the reactance of line $(i,j) \in \mathcal{L}_n$, then the power flow p_{nijt} is given by:

$$p_{nijt} = \frac{V_{nit} V_{njt}}{X_{nij}} \left(\theta_{nit} - \theta_{njt} \right) \quad \forall t \in \mathcal{T}, \tag{12}$$

where the decision variable θ_{nit} is the angle of bus i. Further, the power flow p_{nijt} and bus angle θ_{nit} should be within their intervals $[p_{nij}^{min}, p_{nij}^{max}]$ and $[\theta_{nij}^{min}, \theta_{nij}^{max}]$, respectively.

Each agent has the objective of minimizing the following: the total cost of generation, the penalty for under-utilizing the power already purchased, the unused renewable generation, and the unmet demands. Let c_{njt}^g, d_{ijt}^p, d_{ijt}^r, and d_{ijt}^{ℓ} represent the corresponding unit costs, thus, the objective is:

$$\begin{aligned} h_n(x, \omega_n) = \min \sum_{t \in \mathcal{T}_n} \Bigg[& \sum_{j \in \mathcal{G}_n} c_{njt}^g g_{njt} + \sum_{\substack{(i,j) \in \mathcal{I}_n \\ n \ne 0}} d_{ijt}^p u_{ijt}^p \\ & + \sum_{j \in \mathcal{R}_n} d_{njt}^r u_{njt}^r + \sum_{j \in \mathcal{L}_n} d_{njt}^{\ell} u_{njt}^{\ell} \Bigg] \\ s.t. \quad & (3),\ (10), \text{and } (12) \\ & a_{njt} \in \mathcal{A}_n^v. \end{aligned} \tag{13}$$

The arbiter's decision as well as stochastic information (renewable generation) affect only the right-hand side of the above program. The agent subproblem and the arbiter's problem in (2), which is referred to as the first-stage problem, together constitute our MA-SP:

$$\begin{aligned} \min \ & c^\top x + \sum_{n \in \mathcal{N}} v_n \mathbb{E}\{h_n(x, \omega_n)\} \\ \text{s.t.} \ & x \in \mathcal{X}, \end{aligned} \tag{14a}$$

where,

$$\begin{aligned} h_n(x, \omega_n) = \min \ & d_n^\top y_n \\ s.t. \ & W_n y_n \le r_n(\omega_n) - T_n(\omega_n) x, \\ & y_n \ge 0. \end{aligned} \tag{14b}$$

The subproblem (14b) is a succinct representation of the agent problem in (13). We resort to this representation to simplify

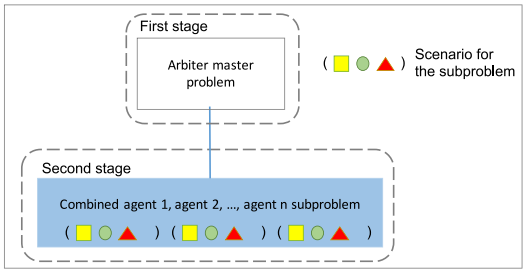

(a) Decision structure of 2-SP

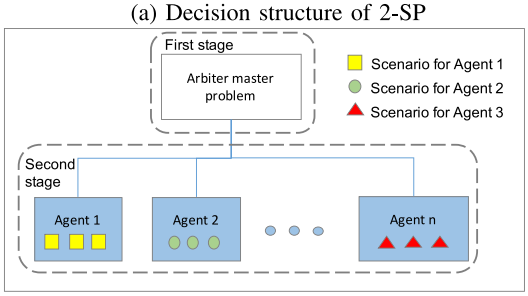

(b) Decision structure of MA-SP

Fig. 2. Decision structures.

the exposition of our algorithm in the next section. Notice that the objective function and constraints are linear functions, the first-stage decisions affect the right-hand side of (14b), and the recourse matrix is independent of uncertainty. Therefore, this formulation is an extension of 2-SP with fixed recourse [30].

III. Algorithm

The formulation introduced in Section II has an arbiter problem where decisions are made before the realization of demand and renewable generation as well as multiple agent problems that provide the recourse costs for the arbiter's decisions. If all the agents can be operated/controlled by a single decision maker, then a combined optimization program can be used to obtain their decisions (shown by the large shaded blue box in Fig. 2(a)). Further, a subproblem scenario is a single vector of observation at all agents. In this setting, the problem can be formulated as a 2-SP. However, the agents have independent decision makers with heterogeneous optimization problems. They are exposed to different stochastic processes. As (14) shows, the proposed MA-SP has a weighted sum of expected recourse functions in the first stage. Each expected recourse function corresponds to an independent agent subproblem (shown by separate and small shaded blue boxes in Fig. 2(b)). In this case, every agent only observes scenarios from its stochastic process. The presence of multiple subproblems distinguishes our MA-SP from the classical formulation which only has one expected recourse function.

The classical 2-SPs are well studied in the literature. The uncertainty is represented using a set of scenarios and the expectation function is computed using the probability associated with each scenario. When the set of scenarios is not readily available, the expectation function is replaced by its sample average approximation (SAA):

$$H(x) = \frac{1}{M}\sum_{i=1}^{M} h\left(x, \omega^i\right), \tag{15}$$

where M is the number of scenarios. Several algorithms, notably, Benders' decomposition [31], Dantzig-Wolfe decomposition [32], and progressive hedging [33], can be used to solve the SAA. These algorithms build lower bounding piecewise linear functions by solving a subproblem for each scenario from a set of scenarios selected a priori. For large-scale problems and/or problems with a large set of scenarios, such enumeration can prove to be computationally challenging. This is particularly the case in power systems with significant renewable integration. For such problems, sequential sampling-based bundling algorithms, such as 2-SD, have proven to be effective [34]. Recent work [35] has illustrated the advantages of sequential sampling over SAA for a wide range of applications. Motivated by these observations, we adopt a modified 2-SD solution approach to tackle our MA-SP.

Our solution approach, which we refer to as multi-agent stochastic decomposition (MA-SD), is an extension of 2-SD when multiple subproblems exist. The principal idea is to use a separate sample mean function to approximate the expected recourse function for each agent in (2):

$$H_n^k(x) = \frac{1}{k}\sum_{j\in\Omega_n^k} h_n\left(x, \omega_n^j\right) \qquad \forall n \in \mathcal{N}. \tag{16}$$

Note that the above sample mean is based on the current set of observations Ω_n^k. In any iteration k, these sample mean functions are updated by sequentially sampling scenarios (ω_n^k) from their respective stochastic processes and updating the observation set Ω_n^k. For the current arbiter decision x^k and newly sampled observation ω_n^k, the subproblem for agent-n is solved. Let π_n^{kk} denote the corresponding optimal dual solution. This solution is added to the set of previously encountered dual solutions, Π_n^k. For the remaining observations $\omega_n^j \in \Omega_n^k$, a dual solution π_n^{kj} is identified in Π_n^k, which provides the best lower bound at x^k. Using these dual solutions $\{\pi_n^{kj}\}_{j=1}^k$, we compute a lower bounding affine function for the k^{th} sample mean function $H_n^k(x)$:

$$H_n^k(x) \geq \underbrace{\frac{1}{k}\sum_{j=1}^{k}\left(\pi_n^{kj}\right)^\top\left[r_n\left(\omega_n^j\right) - T_n\left(\omega_n^j\right)x\right]}_{:=\ell_n^k\left(x,\Omega_n^k\right)}. \tag{17}$$

Note that $H_n^k(x)$ approaches the expectation function as $k \to \infty$. Further, the affine function ℓ_n^j computed in iteration $j(< k)$ is a lower bound for H_n^j, and not necessarily for H_n^k.

Therefore, the previously generated affine functions are updated by multiplying ℓ_n^j by the factor $\frac{j}{k}$. Using these, the piecewise linear approximation [36] of the expected recourse function of agent n is given by:

$$L_n^k(x) = \max_{j=1,\ldots,k}\left\{\frac{j}{k} \times \ell_n^j\left(x, \Omega_n^k\right)\right\}. \tag{18}$$

Approximations of (18) are weighted and aggregated across all agents to form the first-stage problem, which is given by

$$\min\left\{c^\top x + \sum_{n=1}^{N} v_n L_n^k(x) + \frac{\sigma^k}{2}\left\|x - \hat{x}^k\right\|^2 \mid x \in \mathcal{X}\right\}, \tag{19}$$

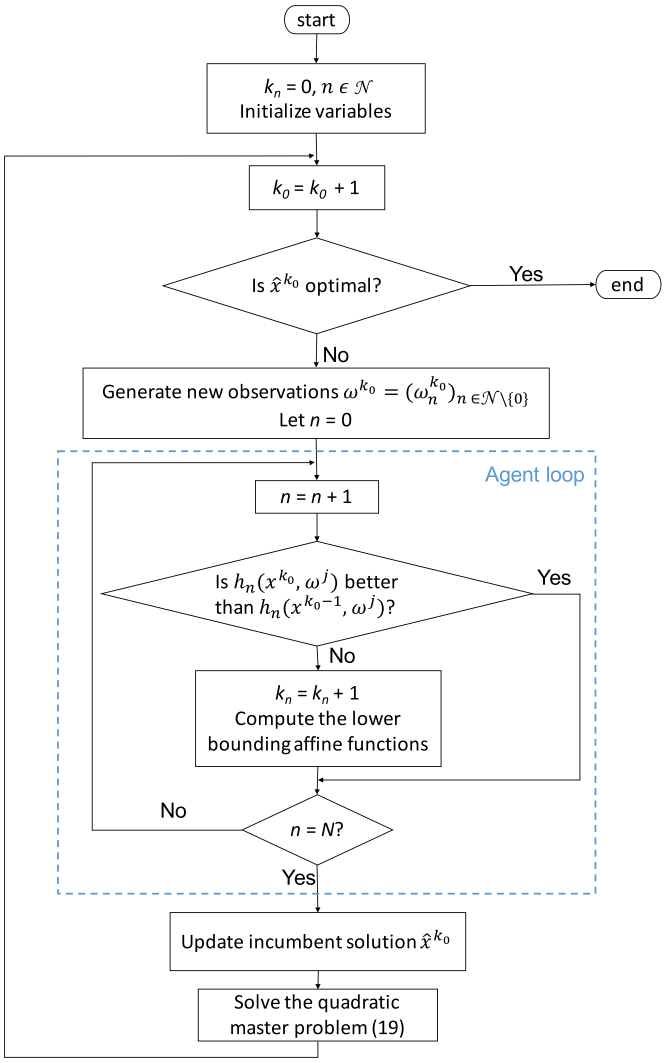

Fig. 3. Flowchart of the MA-SD algorithm.

for a given parameter $\sigma^k > 0$. The optimal solution of the above problem x^{k+1} will be used in the subsequent iteration. Notice the use of a regularization term, centered around the incumbent solution $\hat{x}^k$, in the objective function. This term is included to stabilize our sampling-based approach. We refer the reader to [35] for a detailed exposition of incumbent updates and convergence properties of our approach. Fig. 3 provides a flowchart representation of our algorithm.

Since each agent is exposed to an independent stochastic process, one should expect that different number of scenarios is required to characterize the uncertainty. Further, since the optimization problem is different at every agent, the number of extreme points (dual solutions) relevant to approximate the cost function is also different. In this regard, our stopping rules are based on in-sample as well as out-sample tests for stability of the observation set Ω_n^k and dual solution set Π_n^k. We refer the reader to [35] for more details. Due to the heterogeneous nature of decision processes, different agents might satisfy the stopping criteria at different iterations. Further, since the algorithm allows samples to be added sequentially during the optimization process, such a sequence can be obtained from state-of-the-art simulators that are often used by power system operators.

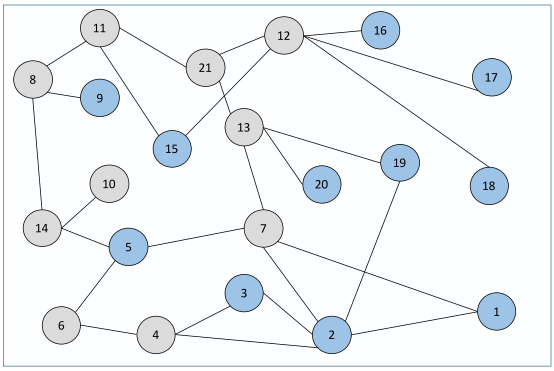

Fig. 4. Network topology of WECC-240.

IV. Computational Experiments

For our computational experiments, we used the WECC-240 data set obtained from [37]. The data consists of a detailed description of network topology, generator location, and capacity. In the data set, all 240 buses, which are located in the western part of the U.S., are originally partitioned into 21 areas (see Fig. 4). We decomposed this data set into one main grid (shown in gray) connected to $N = 10$ MGs (shown in blue). The renewable generation data was extracted from the Western Wind and Solar Integration Study [38] based on the generators' geographical locations. This data was scaled to ensure 15% renewable penetration at each MG and used to build a model that provides a stream of simulated outcomes for renewable generation. We used the demand data in the WECC data set to create the instance, and the buses with flexible demand were selected randomly from the set of all load locations. We adopted the generation costs provided by [39]. Table I presents the details of this power system. In our computational study, we set the time horizon $T = 24$ hours.

All algorithms were implemented in the C programming language on a 64-bit Intel core i7-4770 CPU @3.4GHz $\times$ 8 machine with 32 GB Memory. All linear and quadratic programs were solved using CPLEX callable subroutines. In all our experiments, we begin by using an optimization process to identify an optimal solution for the arbiter and the corresponding prediction value. Note that this prediction value is an estimate of the lower bound for the original optimization problem. This is followed by a verification phase where the arbiter's solution is fixed, and agents (MGs) subproblems are simulated using independent and identically distributed observations. The objective functions obtained are used to build a confidence interval (CI) of the upper bound estimate for each agent's expected recourse function. The CI for the arbiter objective function value is the aggregate based on the weighted sum of individual agent objective values.

A. Comparison of Decision Structures

We start by comparing our MA-SP with the classical 2-SP. While MA-SP includes a separate subproblem for each agent, the 2-SP considers a subproblem that aggregates together the decision processes of all agents. The uncertainty in 2-SP is captured by a single random vector, say

TABLE I
DETAILS OF THE WECC-240 POWER SYSTEM

Agent	Weights	# of Buses	# of Lines	# of Generators		# of Demand Locations		Energy Management Settings				
n	v_n	$\lvert\mathcal{B}_n\rvert$	$\lvert\mathcal{L}_n\rvert$	$\lvert\mathcal{G}_n\rvert$	$\lvert\mathcal{R}_n\rvert$	Fixed ($\lvert\mathcal{D}_n^f\rvert$)	Flexible ($\lvert\mathcal{D}_n^v\rvert$)	$\lvert\mathcal{V}_n^i\rvert$	$\lvert\mathcal{V}_n^h\rvert$	$\lvert\mathcal{V}_n^b\rvert$	$\lvert\mathcal{V}_n^p\rvert$	$\lvert\mathcal{V}_n^a\rvert$
0	1	81	100	24	0	40	0	0	0	0	0	0
1	1	21	24	15	3	7	6	2	1	1	1	1
2	1	2	1	2	1	0	1	0	0	0	0	1
3	1	15	18	2	1	5	7	2	1	1	2	1
4	1	14	17	3	1	3	7	2	1	0	2	2
5	1	29	36	5	1	12	11	3	1	2	3	2
6	1	33	41	16	7	5	10	3	1	1	2	3
7	1	6	5	5	1	0	3	2	0	0	0	1
8	1	29	36	17	4	11	10	2	3	1	3	1
9	1	5	4	3	1	1	2	0	0	0	1	1
10	1	5	5	3	1	1	3	1	0	0	1	1

TABLE II
COMPARISON BETWEEN 2-SP AND MA-SP

Structure	# of optimization programs	Time per iter. (s)	Prediction value ($)	95% C.I.	p-value
2-SP	708	18.682	43,760,652	[43,499,527, 44,103,080]	-
MA-SP	670	9.849	43,951,145	[43,534,253, 44,252,131]	0.7008

$\tilde{\omega}_t = (\tilde{\omega}_{1t}, \tilde{\omega}_{2t}, \ldots, \tilde{\omega}_{Nt})$. The first-stage problem in both these formulations remains the same. We used the 2-SD algorithm to optimize the 2-SP. These results are summarized in TABLE II.

Note that the total costs (i.e., prediction value) for MA-SP is within 0.5% of that predicted by the benchmark 2-SD algorithm. This indicates that the objective function value estimated by considering a separate sampling procedure for each agent is statistically similar to when a single stream of samples is used. The verification CIs, on the other hand, provide us with a tool to compare the solutions generated from the formulations. We accomplished this by testing the following hypothesis: the solutions from the two formulations are statistically indistinguishable. The p-value associated with this hypothesis test is 0.7008, which is greater than 0.05. It indicates that the hypothesis cannot be rejected at a 0.95 significance level.

The first column of TABLE II shows that solving an MA-SP requires a smaller number of iterations than solving a 2-SP (670 vs. 708). In 2-SP, the number of scenarios (of random vector $\tilde{\omega}_t$) is equal to the number of optimization programs, while, for solving the MA-SP, the number of scenarios encountered by each agent (i.e., random variable $\tilde{\omega}_{nt}$) is different. We will discuss it in the following sub-section. The average time taken to complete an iteration of each algorithm is presented in TABLE II as well. Since MA-SP decomposes the subproblems into smaller linear programs, the computational requirements are lower when compared to 2-SP where a significantly larger linear program is solved. Therefore, the average time taken for an iteration in 2-SD is twice as much as MA-SD. The separation of sampling procedures and the computational advantage make the MA-SP setup suitable for parallel computing environments. We are currently working on an implementation suitable for such environments, and the results will be reported in future publications.

B. Comparison of Cut Formation Procedures

The expected recourse function for each agent is approximated using lower bounding affine functions as described in Section III. These approximations are included in the master problem as linear functional constraints [40]. This implies that the size of the master problem grows by N (number of agents/MGs) in every iteration that increases the computational burden of solving quadratic programs. Alternatively, one may aggregate these affine functions as:

$$\bar{\alpha} = \sum_{n=1}^{N} v_n \alpha_n; \qquad \bar{\beta} = \sum_{n=1}^{N} v_n \beta_n, \tag{20}$$

where (α_n, β_n) are coefficients of individual affine functions for $n = 1, \ldots, N$, and $(\bar{\alpha}, \bar{\beta})$ are those for the aggregated affine function. This choice motivates the next set of experiments where we compare the MA-SD(m) and MA-SD(a) procedures. In MA-SD(m), N affine functions are added in every iteration, and a single aggregated function is added in MA-SD(a). The results of MA-SD(a) and MA-SD(m) are shown in TABLE III and TABLE IV, respectively.

These results indicate that, while the number of quadratic master programs solved is higher in the case of MA-SD(a) when compared to MA-SD(m), the corresponding running time is lower. This can be attributed to the larger size of the master problem in the MA-SD(m). As before, we can compare the prediction and verification values to establish the similarity between the two approaches. The difference in prediction values of the two approaches is around 0.3%. We also conducted a hypothesis test that there is no difference between the solutions obtained from these two algorithms. The p-value of 0.9751 (> 0.05) indicates that we cannot reject the null hypothesis of statistically indistinguishable arbiter solutions.

The results in the two tables showcase one of the principal features of our solution approach, viz. the distributed nature of our sequential sampling procedure. Since each agent

TABLE III
RESULTS OF MA-SD(a)

Agents	# of optimization programs	Time per iter. (s)	Prediction value ($)	Mean	U.B. Estimate Std. dev.	95% C.I.
master	670	9.849	43,951,145	43,893,192	5,788,250	[43,534,253, 44,252,131]
0	369	0.012	0.007	0.007	0.000	[0.007, 0.007]
1	301	0.002	8,998,948	8,997,077	150,725	[8,987,730, 9,006,424]
2	475	0.002	8,755	8,749	694	[8,706, 8,792]
3	359	0.004	2,139,078	2,140,098	91,629	[2,134,416, 2,145,780]
4	343	0.004	2,076,822	1,994,509	946,845	[1,935,793, 2,053,224]
5	368	0.015	783,400	772,364	310,294	[753,122, 791,606]
6	275	0.014	4,263,634	4,205,003	2,863,423	[4,027,438, 4,382,569]
7	374	0.003	5,228,603	5,350,485	4,560,169	[5,067,701, 5,633,268]
8	265	0.006	6,692,126	6,665,261	1,822,699	[6,552,233, 6,778,290]
9	323	0.001	206,019	203,565	101,432	[197,275, 209,855]
10	351	0.002	645,443	640,605	220,237	[626,947, 654,262]

TABLE IV
RESULTS OF MA-SD(m)

Agents	# of optimization programs	Time per iter. (s)	Prediction value ($)	Mean	U.B. Estimate Std. dev.	95% C.I.
master	435	15.957	44,066,906	43,885,109	5,796,994	[43,525,628, 44,244,591]
0	311	0.012	0.004	0.004	0.000	[0.004,0.004]
1	279	0.002	8,657,521	8,654,370	142,600	[8,645,527, 8,663,213]
2	433	0.002	8,824	8,790	723	[8,745, 8,834]
3	375	0.003	2,144,479	2,146,895	98,548	[2,140,784, 2,153,006]
4	346	0.004	2,053,008	2,008,981	958,127	[1,949,566, 2,068,396]
5	393	0.019	800,002	774,888	311,272	[755,585, 794,190]
6	267	0.017	4,426,207	4,213,061	2,870,708	[4,035,044, 4,391,078]
7	314	0.002	5,173,337	5,341,604	4,560,194	[5,058,819, 5,624,389]
8	263	0.007	7,025,171	6,965,143	1,830,957	[6,851,602, 7,078,684]
9	317	0.001	197,412	192,457	92,595	[186,715, 198,199]
10	281	0.001	648,653	646,629	222,103	[632,856, 660,402]

is exposed to stochastic processes with different characteristics (mean, variance, etc.), the number of samples required to satisfactorily approximate the expected recourse function is also different. These numbers can be seen in the first column of TABLE III and TABLE IV for each method, respectively. For sample-based stochastic programming models, it is not guaranteed that the prediction value falls within the verification CI. However, when it does, then the solutions can be accepted with greater confidence. The arbiter solution satisfies this condition as the aggregated prediction value falls within the verification CI for both methods proposed. (See the row corresponding to "master" in TABLE III and TABLE IV.) While this solution is statistically acceptable to the aggregated optimization problem, it might not be the case for individual agents (e.g., agent 4 in the MA-SD(a) method). Such behavior can be attributed to the fact that our approach seeks solutions that are optimal across all and not necessarily individual agents. In the remaining experiments, we will use MA-SD(a) as our method of choice to solve MA-SPs.

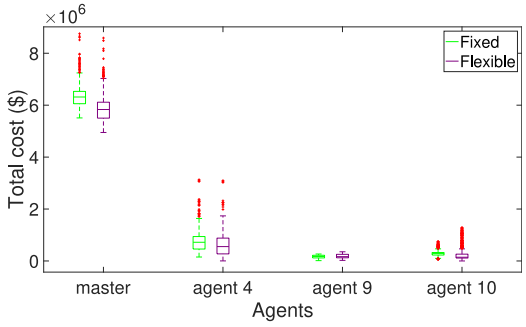

Fig. 5. Objective values of the arbiter and agents.

C. Study the Impacts of the Network Constraints

The formulation presented in Section II considers a DC approximation of the power flow constraints (10). Power flow on line (i, j) is bounded by the line capacity $[p_{nij}^{min}, p_{nij}^{max}]$. In order to study the impact of these constraints, we created instances without power flows ("NoNetwork"), uncapacitated power flows ("Uncapacitated"), and capacitated power flows ("Capacitated"). In the "NoNetwork" instance, system-wide power balance was ensured by including:

$$\sum_{j \in \mathcal{G}_n} g_{njt} = \sum_{j \in \mathcal{D}_n \bigcup \mathcal{R}_n} \partial \bar{D}_{njt} - \sum_{(i,j) \in \mathcal{I}_n} b_{ijt} \quad \forall t \in \mathcal{T}_n, \qquad (21)$$

where $\partial \bar{D}_{njt}$ is the net demand computed using customer demand ($\mathcal{D}_n$) and renewable generation ($\mathcal{R}_n$) in all agents $n \in \mathcal{N}$. The results are shown in TABLE V. Since the

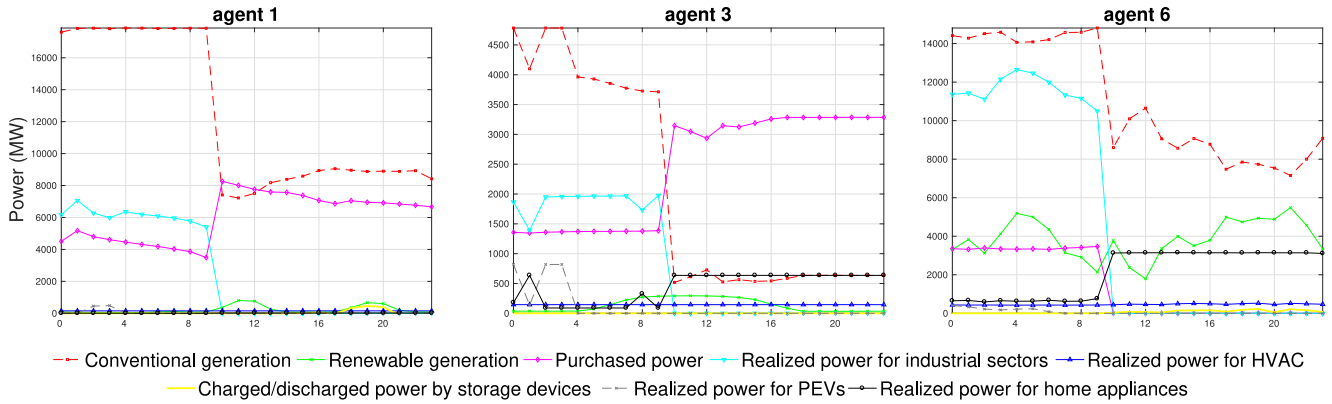

Fig. 6. Mean agent response for different energy management settings.

TABLE V
SOLUTION RESULTS OF VARIOUS NETWORK CONSTRAINTS

Instances	Prediction value ($)	95% C.I.	p-value
NoNetwork	37,138,279	[36,930,348, 37,366,901]	-
Uncapacitated	37,132,967	[36,926,762, 37,363,174]	0.9815
Capacitated	43,951,145	[43,534,253, 44,252,131]	0

TABLE VI
SOLUTION METHOD COMPARISON (FIXED AND FLEXIBLE)

Instances	Prediction Value($)	Conventional Generation (MW)	Selling Power (MW)	95% C.I.
Fixed	6,360,378	412,471	108,236	[6,316,083, 6,364,164]
Flexible	4,879,788	376,211	71,986	[4,818,633, 4,867,403]

"NoNetwork" and "Uncapacitated" instances are relaxations of the original problem, the total cost is lower than the "Capacitated" instance. Moreover, the solution obtained for "Capacitated" is significantly different from the other instances (indicated by low p-value). It is interesting to notice that the solutions and values from "NoNetwork" and "Uncapacitated" instances are statistically indifferent. This indicates that the capacity on power flows is more critical than the power flow approximation (12), at least for our data set.

D. Energy Management Study

The formulation of the power system presented in Section II permitted different energy management settings to be included at agents. A main feature of these settings was the flexibility to schedule demand in a way that reduces overall system costs by efficiently managing their schedule with availabilities of renewable resources. In order to quantify the cost savings, we designed an experiment to compare a system with/without such flexible demands. Our experiment used two small instances comprised of the main grid and agents 4, 9, and 10 (all without storage devices)—one instance has inflexible customer demands and the other instance allows flexibility. All renewable generation scenarios used in this experiment are from the same data set as before.

The prediction and verification results are summarized in TABLE VI. The prediction values indicate that incorporating flexibility in energy management systems helps to reap more benefits from renewable resources and thereby results in cost savings (7.9%) for the system. This decrease in cost can be attributed to an 2.7% reduction in the conventional generation and a 10.4% reduction in the total amount of energy sold by the main grid. Further, from Fig. 5, we see that both the main grid and agents can reduce their total costs by allowing demands to be flexible. However, the cost reduction is more prominent in the main grid than individual agents.

E. Response of Flexible Demands

In this experiment, we study the response of flexible demands to fluctuations in renewable generation over the planning horizon. The optimal first-stage solution identified by MA-SD(a) is treated as an input to the individual agent problem. The decision process of each agent is simulated by solving an optimization problem using independent Monte-Carlo samples. Some key observations are discussed here.

Fig. 6 shows the mean responses over 1000 samples for different settings during a day for agents 1, 3, and 6. The power purchased (which is a part of arbiter decisions), local conventional generation, and renewable generation are utilized to satisfy both flexible and fixed demand of an agent. During time window [0, 9], the requirements of industrial facilities dominate the power consumption and drive a high level of local conventional generation for all the three agents. In time period 10, when the industrial facilities stop operating, the local conventional generation reduces dramatically while the purchased power increases for agents 1 and 3 only.

Another interesting observation from Fig. 6 is that industrial and home appliances demand realization trends complement one another. For example, when industrial demand decreases at the end of time period 9, the demand of home appliances is scheduled to be met. This behavior can be attributed to the fact that home appliances are allowed to operate over a longer time window as compared to industrial demand, which makes them more flexible. Similar complementary behavior was observed between conventional and renewable generation. We also can

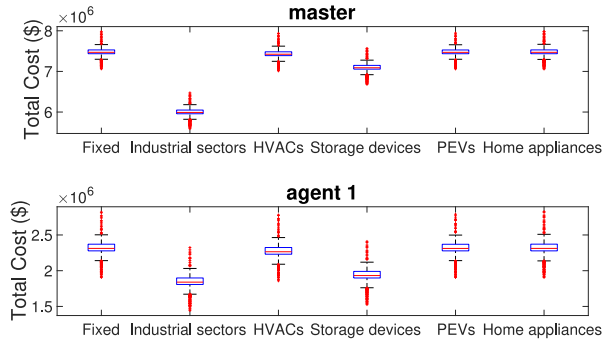

Fig. 7. Sensitivity analysis of energy management settings.

see from Fig. 6 that excess renewable energy is stored (e.g., in $t \geq 10$ in agent 6) for future usage. While the realized power for the HVACs is constant for a majority of agents, this is not the case for agent 6 (see Fig. 6). This is due to the presence of renewable resources with higher variability at this agent when compared to others. Both HVACs and storage devices help in smoothing this variability.

Further, we conducted sensitivity analysis of different type of flexible demands to investigate the effect of their variations on agents' total costs. The power system in this experiment comprises only one agent (agent 1) and the main grid. Our benchmark is to set all demands as fixed and no storage devices installed. Then we only allowed one type of energy management setting to be flexible. We conducted the same experiment for the rest of the settings. When storage devices are used, all other settings are not allowed to be flexible. The total costs for the main grid and agent 1 are shown in Fig. 7. It was observed that the total cost savings are proportional to the power demand. This seems to be the case for industrial sectors in Fig. 7. The figure also illustrates the role of storage devices in reducing total costs by moving energy from time periods of abundant generation to periods of low generation (also see Fig. 6).

V. Conclusion

In this paper, we presented a stochastic optimization framework that captures interactions between (a) a centralized arbiter in the main grid and (b) multiple agents with heterogeneous objectives and constraints in MGs that utilize various energy management settings. We investigated the response of each agent to intermittent renewable resources by extending the classical 2-SP model to include multiple subproblems. To the best of our knowledge, this is the first study that investigates multiple subproblems with heterogeneous decisions and stochastic processes in the second-stage. We developed stochastic decomposition-based algorithms to solve the proposed large-scale problem. The statistical results showed that our algorithm can provide reliable overall cost estimates to the proposed problem with 50% less running time as compared to the benchmark 2-SD approach. Our algorithm used two different approximation approaches: agent cuts (MA-SD(m)) and aggregated cuts (MA-SD(a)). Both these approaches yield statistical comparable results, but the aggregated approach is computationally more efficient. The results implemented with and without allowing flexible demands show that the total operational costs can be reduced significantly when customer demand is flexible by effective utilization of the renewable resources. Our experiments show that cost reductions are more prominent in the main grid than at individual agents. The sensitivity analysis reveals that the flexibility in the industrial sector has the potential to contribute the most towards the total cost reduction. The results also indicate storage devices play a critical role in cost reductions. While the inclusion of power flow equations increases the computational requirements, they are necessary to identify system congestion. This is highlighted by the increase in total cost when flow balance constraints are considered in the proposed MA-SP. Finally, we studied how the activities of these flexible demands fluctuate with variations of renewable generations during a day.

The structure of our algorithm involves solving several independent subproblems (corresponding to MGs). This structure is naturally fit for an implementation of distributed/parallel computing, which will be taken up as part of our future study. In a smart grid, MGs not only are buyers but also can sell power back to the main grid to increase utilization of renewable energy over the entire power system. Furthermore, they are allowed to make transactions with other MGs in the system as well. These features will also be addressed in our future work.

References

[1] Y.-H. Chen, S.-Y. Lu, Y.-R. Chang, T.-T. Lee, and M.-C. Hu, "Economic analysis and optimal energy management models for microgrid systems: A case study in Taiwan," *Appl. Energy*, vol. 103, pp. 145–154, Mar. 2013.

[2] P. Basak, S. Chowdhury, S. H. nee Dey, and S. P. Chowdhury, "A literature review on integration of distributed energy resources in the perspective of control, protection and stability of microgrid," *Renew. Sustain. Energy Rev.*, vol. 16, no. 8, pp. 5545–5556, 2012.

[3] R. H. Lasseter, "Microgrids," in *Proc. IEEE Power Eng. Soc. Win. Meeting*, vol. 1. 2002, pp. 305–308.

[4] A. Zakariazadeh, S. Jadid, and P. Siano, "Smart microgrid energy and reserve scheduling with demand response using stochastic optimization," *Int. J. Elect. Power Energy Syst.*, vol. 63, pp. 523–533, Dec. 2014.

[5] T. Ackermann, G. Andersson, and L. Söder, "Distributed generation: A definition," *Elect. Power Syst. Res.*, vol. 57, no. 3, pp. 195–204, 2001.

[6] C. Bueno and J. A. Carta, "Wind powered pumped hydro storage systems, a means of increasing the penetration of renewable energy in the Canary Islands," *Renew. Sustain. Energy Rev.*, vol. 10, no. 4, pp. 312–340, 2006.

[7] H. Gangammanavar and S. Sen, "Two-scale stochastic optimization framework for controlling distributed storage devices," *IEEE Trans. Smart Grid*, to be published, doi: 10.1109/TSG.2016.2616881.

[8] M. Marzband, N. Parhizi, M. Savaghebi, and J. M. Guerrero, "Distributed smart decision-making for a multimicrogrid system based on a hierarchical interactive architecture," *IEEE Trans. Energy Convers.*, vol. 31, no. 2, pp. 637–648, Jun. 2016.

[9] A. R. Malekpour and A. Pahwa, "Stochastic energy management in distribution systems with correlated wind generators," *IEEE Trans. Power Syst.*, vol. 32, no. 5, pp. 3681–3693, Sep. 2017.

[10] K. Boroojeni *et al.*, "A novel cloud-based platform for implementation of oblivious power routing for clusters of microgrids," *IEEE Access*, vol. 5, pp. 607–619, 2017.

[11] Z. Wang, B. Chen, J. Wang, M. M. Begovic, and C. Chen, "Coordinated energy management of networked microgrids in distribution systems," *IEEE Trans. Smart Grid*, vol. 6, no. 1, pp. 45–53, Jan. 2015.

[12] H. S. V. S. K. Nunna and S. Doolla, "Multiagent-based distributed-energy-resource management for intelligent microgrids," *IEEE Trans. Ind. Electron.*, vol. 60, no. 4, pp. 1678–1687, Apr. 2013.

[13] T. Logenthiran, D. Srinivasan, and A. M. Khambadkone, "Multi-agent system for energy resource scheduling of integrated microgrids in a distributed system," *Elect. Power Syst. Res.*, vol. 81, no. 1, pp. 138–148, 2011.
[14] T. Dai and W. Qiao, "Trading wind power in a competitive electricity market using stochastic programing and game theory," *IEEE Trans. Sustain. Energy*, vol. 4, no. 3, pp. 805–815, Jul. 2013.
[15] S. W. Wallace and S.-E. Fleten, "Stochastic programming models in energy," *Handbooks Oper. Res. Manag. Sci.*, vol. 10, pp. 637–677, 2003, doi: 10.1016/S0927-0507(03)10010-2.
[16] A. Sheikhi, A. Maani, and A. M. Ranjbar, "Evaluation of intelligent distribution network response to plug-in hybrid electric vehicles," in *Proc. IEEE Grenoble PowerTech (POWERTECH)*, Grenoble, France, 2013, pp. 1–6.
[17] D. T. Nguyen and L. B. Le, "Optimal energy management for cooperative microgrids with renewable energy resources," in *Proc. IEEE Int. Conf. Smart Grid Commun. (SmartGridComm)*, Vancouver, BC, Canada, 2013, pp. 678–683.
[18] Y. M. Ding, S. H. Hong, and X. H. Li, "A demand response energy management scheme for industrial facilities in smart grid," *IEEE Trans. Ind. Informat.*, vol. 10, no. 4, pp. 2257–2269, Nov. 2014.
[19] G. Goddard, J. Klose, and S. Backhaus, "Model development and identification for fast demand response in commercial HVAC systems," *IEEE Trans. Smart Grid*, vol. 5, no. 4, pp. 2084–2092, Jul. 2014.
[20] N. Li, L. Chen, and S. H. Low, "Optimal demand response based on utility maximization in power networks," in *Proc. IEEE Power Energy Soc. Gen. Meeting*, Detroit, MI, USA, 2011, pp. 1–8.
[21] Z. Chen, L. Wu, and Y. Fu, "Real-time price-based demand response management for residential appliances via stochastic optimization and robust optimization," *IEEE Trans. Smart Grid*, vol. 3, no. 4, pp. 1822–1831, Dec. 2012.
[22] P. Zhao, S. Suryanarayanan, and M. G. Simoes, "An energy management system for building structures using a multi-agent decision-making control methodology," *IEEE Trans. Ind. Appl.*, vol. 49, no. 1, pp. 322–330, Jan./Feb. 2013.
[23] R. de Dear and G. S. Brager, "The adaptive model of thermal comfort and energy conservation in the built environment," *Int. J. Biometeorol.*, vol. 45, no. 2, pp. 100–108, 2001.
[24] D. J. Sailor and A. A. Pavlova, "Air conditioning market saturation and long-term response of residential cooling energy demand to climate change," *Energy*, vol. 28, no. 9, pp. 941–951, 2003.
[25] Y. Agarwal *et al.*, "Occupancy-driven energy management for smart building automation," in *Proc. 2nd ACM Workshop Embedded Sens. Syst. Energy Efficiency Build.*, Zürich, Switzerland, 2010, pp. 1–6.
[26] A. Etxeberria, I. Vechiu, H. Camblong, J. M. Vinassa, and H. Camblong, "Hybrid energy storage systems for renewable energy sources integration in microgrids: A review," in *Proc. Conf. IPEC*, Singapore, 2010, pp. 532–537.
[27] P. Denholm, E. Ela, B. Kirby, and M. Milligan, "The role of energy storage with renewable electricity generation," Nat. Renew. Energy Lab., Golden, CO, USA, Tech. Rep. NREL/TP-6A2-47187, 2010.
[28] R. Sioshansi, P. Denholm, and T. Jenkin, "Market and policy barriers to deployment of energy storage," *Econ. Energy Environ. Policy*, vol. 1, no. 2, pp. 47–63, 2012.
[29] A. L. Motto, F. D. Galiana, A. J. Conejo, and J. M. Arroyo, "Network-constrained multiperiod auction for a pool-based electricity market," *IEEE Trans. Power Syst.*, vol. 17, no. 3, pp. 646–653, Aug. 2002.
[30] J. R. Birge and F. Louveaux, *Introduction to Stochastic Programming*. New York, NY, USA: Springer, 2011.
[31] J. F. Benders, "Partitioning procedures for solving mixed-variables programming problems," *Numerische Mathematik*, vol. 4, no. 1, pp. 238–252, 1962.
[32] G. B. Dantzig and P. Wolfe, "Decomposition principle for linear programs," *Oper. Res.*, vol. 8, no. 1, pp. 101–111, 1960.
[33] R. T. Rockafellar and R. J.-B. Wets, "Scenarios and policy aggregation in optimization under uncertainty," *Math. Oper. Res.*, vol. 16, no. 1, pp. 119–147, 1991.
[34] H. Gangammanavar, S. Sen, and V. M. Zavala, "Stochastic optimization of sub-hourly economic dispatch with wind energy," *IEEE Trans. Power Syst.*, vol. 31, no. 2, pp. 949–959, Mar. 2015.
[35] S. Sen and Y. Liu, "Mitigating uncertainty via compromise decisions in two-stage stochastic linear programming: Variance reduction," *Oper. Res.*, vol. 64, no. 6, pp. 1422–1437, 2016.
[36] J. L. Higle and S. Sen, "Finite master programs in regularized stochastic decomposition," *Math. Program.*, vol. 67, nos. 1–3, pp. 143–168, 1994.
[37] J. E. Price and J. Goodin, "Reduced network modeling of WECC as a market design prototype," in *Proc. IEEE Power Energy Soc. Gen. Meeting*, Detroit, MI, USA, 2011, pp. 1–6.
[38] *Western Wind and Solar Integration Study*, Nat. Renew. Energy Lab., Golden, CO, USA, accessed: Nov. 26, 2016. [Online]. Available: http://www.nrel.gov/grid/wwsis.html
[39] *Levelized Cost and Levelized Avoided Cost of New Generation Resources in the Annual Energy Outlook*, U.S. Energy Inf. Admin., Washington, DC, USA, 2015, accessed: Nov. 26, 2016. [Online]. Available: http://www.eia.gov/outlooks/archive/aeo
[40] J. L. Higle and S. Sen, "Duality and statistical tests of optimality for two stage stochastic programs," *Math. Program.*, vol. 75, no. 2, pp. 257–275, 1996.

Shasha Wang received the B.S. and M.S. degrees in chemical engineering from the East China University of Science and Technology, Shanghai, China, in 2008 and 2011, respectively, and the M.S. degree in industrial engineering from Clemson University in 2015, where she is currently pursuing the Ph.D. degree with the Industrial Engineering Department. Her research interests are focused on stochastic programming for large-scale planning and scheduling problems integrated with on-site renewable energy resources.

Harsha Gangammanavar received the M.S. degree in electrical engineering and the Ph.D. degree in operations research from Ohio State University in 2009 and 2013, respectively. He is an Assistant Professor with the Department of Engineering Management, Information, and Systems, Southern Methodist University. He has held the position of Post-Doctoral Fellow in industrial engineering with Clemson University and a Visiting Assistant Professor with the Daniel J. Epstein Department of Industrial and Systems Engineering, University of Southern California. His research interests are focused on stochastic optimization and its application in power systems planning and operations.

Sandra D. Ekşioğlu is an Associate Professor of industrial engineering with Clemson University. Her expertise is in the areas of operations research, network optimization, and algorithmic development. She uses these tools to develop models and solution algorithms for solving large-scale problems that arise in the areas of transportation, energy, and supply chain. She is an active member of the Institute for Operations Research and the Management Sciences, the Institute of Industrial and Systems Engineers, and the American Society for Engineering Education.

Scott J. Mason received the bachelor's and master's degrees from the University of Texas at Austin and the Ph.D. degree in industrial engineering from Arizona State University. He is the Fluor Endowed Chair in supply chain optimization and logistics and a Professor of industrial engineering with Clemson University. He is the Chair of the SmartState Center of Economic Excellence in Supply Chain Optimization and Logistics, where he is responsible for developing and maintaining active research relationships with both private and public-sector organizations to foster economic development, increased efficiencies, and job creation in the state of South Carolina. He spent ten years with the Department of Industrial Engineering, University of Arkansas. His research focuses on developing effective optimization-based solutions for planning, scheduling, and controlling large-scale supply chain systems and networks. He is a fellow of the Institute for Industrial Engineers and a member of the Institute for Operations Research and the Management Sciences.